2014 IEEE International Conference on Robotics & Automation (ICRA)
Hong Kong Convention and Exhibition Center
May 31 - June 7, 2014. Hong Kong, China

Stability Analysis Method Independent of Numerical Integration for Limit Cycle Walking with Constraint on Impact Posture

Fumihiko Asano[1]

Abstract— **This paper proposes the method independent of numerical integration for analyzing the stability of a limit cycle walker that falls down as a 1-DOF rigid body in the same posture. We introduce the model of an underactuated rimless wheel with a torso for analysis and show that the transition function of the state error can be analytically derived from the recurrence formula of kinetic energy immediately before impact. We then investigate the accuracy of the derived solution through comparison with the numerical solutions and discuss how the convergence property changes with respect to the control parameter. Furthermore, we extend the method to an underactuated biped and show that the stability analysis can be conducted in a similar manner without performing numerical simulations.**

I. INTRODUCTION

Recent robotic walkers that are energy efficient and high speed tend to generate a walking gait as a stable limit cycle including discrete events but without adequate consideration of stability assurance. The stability inherent in robotic legged locomotion as a limit cycle with impulse effects was originally discussed by Hosoe et al. [1] They applied a high-gain PD feedback control to a planar linearized limit cycle walker so that it falls down as a 1-DOF rigid body in the same posture immediately before every impact (constraint on impact posture), and showed that the equilibrium point can be determined by conducting iterative calculation of the angular velocity at impact. After that, Grizzle et al. developed more rigorous theory for nonlinear limit-cycle walkers with constraint on impact posture and showed that the stability of the generated gait is equivalent to that of the step-to-step behavior [2].

The authors have also studied the problem [3][4] and recently achieved to derive the analytical solutions to the transition functions of the state error in limit cycle walking with constraint on impact posture [5]. Assuming that the walker achieves the constraint on impact posture by a strictly output following control, we can reduce the redundant return map to a scalar function of the stance angular velocity immediately after impact to the next immediately before impact. The analytical solution of the transition function, $\bar{Q} \in \mathbb{R}$ for the stance phase, enabled us to mathematically calculate the Poincaré return map. It included, however, the steady parameters in the generated gait such as the step period and the angular velocity [3]. The stability of the collision phase on the other hand can be easily proved because the absolute value of the transition function of the state error, $\bar{R} \in \mathbb{R}$, is less than 1. After these investigations, we succeeded in eliminating the step period from $\bar{Q}$ [4]. Finally, we achieved to derive the analytical solution of $\bar{Q}$ for a 1-DOF active walker as a function only of the control parameters [5].

Based on these observations, in this paper we revisit the problem of stability analysis for general limit-cycle walkers with constraint on impact posture and show that it is possible to analyze the stability of the generated gait without numerical integration. First, we introduce an underactuated rimless wheel model for analysis and describe the method for analytically deriving the transition function of the state error. Unlike the previous method [3][4][5], the novel approach for derivation is very easy and is based only on mechanical energy balance. We discuss the accuracy of the analytical $\bar{Q}$ through numerical investigations. Second, we extend the method to an underactuated biped model and show that the stability analysis can be performed in a similar manner as the previous one.

II. PROBLEM FORMULATION

A. Model of Underactuated Rimless Wheel and Linearization of Motion

Fig. 1 shows the model of an underactuated rimless wheel with a torso [6]. This walker consists of an eight-legged symmetrically-shaped rimless wheel (RW) and a torso link. The relative angle between two adjacent leg frames, α, is $\pi/4$ [rad]. The torso link is connected to the RW at the central position and the moment of inertia about the joint is I [kg·m^2].

Let $\boldsymbol{\theta} = \left[\, \theta_1 \ \theta_2 \,\right]^{\mathrm{T}}$ be the generalized coordinate vector.

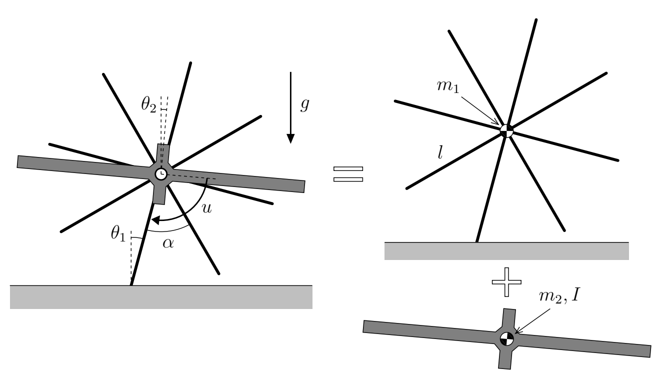

Fig. 1. Model of underactuated rimless wheel with torso

[1]F. Asano is with the School of Information Science, Japan Advanced Institute of Science and Technology, 1-1 Asahidai, Nomi, Ishikawa 923-1292, Japan fasano@jaist.ac.jp

The equation of motion then becomes

$$\begin{bmatrix} Ml^2 & 0 \\ 0 & I \end{bmatrix} \begin{bmatrix} \ddot{\theta}_1 \\ \ddot{\theta}_2 \end{bmatrix} + \begin{bmatrix} -Mgl\sin\theta_1 \\ 0 \end{bmatrix} = \begin{bmatrix} 1 \\ -1 \end{bmatrix} u \quad (1)$$

By linearizing Eq. (1) about $\boldsymbol{\theta} = \dot{\boldsymbol{\theta}} = \mathbf{0}_{2\times 1}$, we get

$$\begin{bmatrix} Ml^2 & 0 \\ 0 & I \end{bmatrix} \begin{bmatrix} \ddot{\theta}_1 \\ \ddot{\theta}_2 \end{bmatrix} + \begin{bmatrix} -Mgl & 0 \\ 0 & 0 \end{bmatrix} \begin{bmatrix} \theta_1 \\ \theta_2 \end{bmatrix} = \begin{bmatrix} 1 \\ -1 \end{bmatrix} u. \quad (2)$$

We denote Eq. (2) as

$$\boldsymbol{M}_0\ddot{\boldsymbol{\theta}} + \boldsymbol{G}_0\boldsymbol{\theta} = \boldsymbol{S}u. \quad (3)$$

Next, we outline the collision dynamics. We assume the followings.

- The walker falls down as a 1-DOF rigid body or achieves the condition of $\dot{\theta}_1 = \dot{\theta}_2$ immediately before the next impact.
- The torso is mechanically locked to the RW during the collision. This condition is mathematically represented by $\dot{\theta}_1^+ = \dot{\theta}_2^+$.

On the above assumptions, the transition equation for the angular velocity becomes

$$\dot{\theta}_1^+ = \dot{\theta}_2^+ = \frac{Ml^2\cos\alpha + I}{Ml^2 + I}\dot{\theta}_1^-. \quad (4)$$

Under this condition, a strict output following control can be achieved as described later. On the other hand, in a steady gait the following relation holds.

$$\dot{\theta}_{1\mathrm{eq}}^+ = \dot{\theta}_{2\mathrm{eq}}^+ = \bar{R}\dot{\theta}_{1\mathrm{eq}}^-, \quad \bar{R} := \frac{Ml^2\cos\alpha + I}{Ml^2 + I} \quad (5)$$

By subtracting Eq. (5) from Eq. (4), we get $\Delta\dot{\theta}_{1(i)}^+ = \bar{R}\Delta\dot{\theta}_{1(i)}^-$ where $\Delta\dot{\theta}_{1(i)}^\pm := \dot{\theta}_{1(i)}^\pm - \dot{\theta}_{1\mathrm{eq}}^\pm$. Therefore $\bar{R}$ is found to be the transition function of the state error for the collision phase, and we can understand that this phase is stable because $|\bar{R}| < 1$ holds.

B. Mechanical Energy for Linearized Model

Define the potential energy corresponding to the linearized model as

$$P(\boldsymbol{\theta}) = P_{\max} + \frac{1}{2}\boldsymbol{\theta}^{\mathrm{T}}\boldsymbol{G}_0\boldsymbol{\theta}, \quad (6)$$

where $P_{\max} = Mgl$ [J] is the maximum potential energy the walker can reach. Eq. (6) is a quadratic approximation of potential energy for the nonlinear model [7]. The kinetic energy is determined as

$$K(\dot{\boldsymbol{\theta}}) = \frac{1}{2}\dot{\boldsymbol{\theta}}^{\mathrm{T}}\boldsymbol{M}_0\dot{\boldsymbol{\theta}}, \quad (7)$$

and this is common to both the nonlinear and the linearized models because the inertia matrix is constant. The total mechanical energy corresponding to the linearized model is then defined as

$$E(\boldsymbol{x}) := K(\dot{\boldsymbol{\theta}}) + P(\boldsymbol{\theta}) = P_{\max} + \frac{1}{2}\boldsymbol{x}^{\mathrm{T}}\boldsymbol{W}_0\boldsymbol{x}, \quad (8)$$

where

$$\boldsymbol{W}_0 := \begin{bmatrix} \boldsymbol{G}_0 & \mathbf{0}_{2\times 2} \\ \mathbf{0}_{2\times 2} & \boldsymbol{M}_0 \end{bmatrix} \in \mathbb{R}^{4\times 4}, \quad \boldsymbol{x} = \begin{bmatrix} \boldsymbol{\theta} \\ \dot{\boldsymbol{\theta}} \end{bmatrix} \in \mathbb{R}^4.$$

$\boldsymbol{W}_0$ is a symmetric matrix and the time-derivative of $E(\boldsymbol{x})$ becomes

$$\frac{\mathrm{d}E(\boldsymbol{x})}{\mathrm{d}t} = \boldsymbol{x}^{\mathrm{T}}\boldsymbol{W}_0\dot{\boldsymbol{x}} = \dot{\boldsymbol{\theta}}^{\mathrm{T}}\left(\boldsymbol{G}_0\boldsymbol{\theta} + \boldsymbol{M}_0\ddot{\boldsymbol{\theta}}\right) = \dot{\boldsymbol{\theta}}^{\mathrm{T}}\boldsymbol{S}u. \quad (9)$$

This property is the same as the nonlinear model.

C. Output Following Control

Let $y := \boldsymbol{S}^{\mathrm{T}}\boldsymbol{\theta} = \theta_1 - \theta_2$ be the control output. We then consider to control y from $-\alpha/2$ to $\alpha/2$ during every stance phase by strictly tracking to the following desired-time trajectory.

$$y_{\mathrm{d}}(t) = \begin{cases} \dfrac{6\alpha}{T_{\mathrm{set}}^5}t^5 - \dfrac{15\alpha}{T_{\mathrm{set}}^4}t^4 + \dfrac{10\alpha}{T_{\mathrm{set}}^3}t^3 - \dfrac{\alpha}{2} & (0 \le t < T_{\mathrm{set}}) \\ \dfrac{\alpha}{2} & (t \ge T_{\mathrm{set}}) \end{cases} \quad (10)$$

This satisfies the following boundary conditions.

$$y_{\mathrm{d}}(0^+) = -\alpha/2, \quad y_{\mathrm{d}}(T_{\mathrm{set}}) = \alpha/2$$
$$\dot{y}_{\mathrm{d}}(0^+) = \dot{y}_{\mathrm{d}}(T_{\mathrm{set}}) = 0, \quad \ddot{y}_{\mathrm{d}}(0^+) = \ddot{y}_{\mathrm{d}}(T_{\mathrm{set}}) = 0$$

By choosing the conditions immediately after impact as $\theta_1^+ = -\alpha/2$, $\theta_2^+ = 0$ and $\dot{\theta}_1^+ = \dot{\theta}_2^+$, we can achieve $y(0^+) = y_{\mathrm{d}}(0^+)$, $\dot{y}(0^+) = \dot{y}_{\mathrm{d}}(0^+)$ and $\ddot{y}(0^+) = \ddot{y}_{\mathrm{d}}(0^+)$. Therefore the walker can strictly control y without including the tracking errors, and PD feedback control is not necessary. The second-order derivative of y with respect to time becomes $\ddot{y} = \boldsymbol{S}^{\mathrm{T}}\ddot{\boldsymbol{\theta}} = \boldsymbol{S}^{\mathrm{T}}\boldsymbol{M}_0^{-1}(\boldsymbol{S}u - \boldsymbol{G}_0\boldsymbol{\theta})$, and the control input, u, for achieving $\ddot{y} = \ddot{y}_{\mathrm{d}}(t)$, i.e. $y \equiv y_{\mathrm{d}}(t)$, can be determined as

$$u = \frac{\ddot{y}_{\mathrm{d}}(t) + \boldsymbol{S}^{\mathrm{T}}\boldsymbol{M}_0^{-1}\boldsymbol{G}_0\boldsymbol{\theta}}{\boldsymbol{S}^{\mathrm{T}}\boldsymbol{M}_0^{-1}\boldsymbol{S}} = \frac{Ml^2 I}{Ml^2 + I}\left(\ddot{y}_{\mathrm{d}}(t) - \omega^2\theta_1\right), \quad (11)$$

where $\omega := \sqrt{g/l}$ [rad/s]. By substituting this into Eq. (2) and extracting the first low, we get

$$\ddot{\theta}_1 = \hat{\omega}^2\theta_1 + \frac{I}{Ml^2 + I}\ddot{y}_{\mathrm{d}}(t), \quad \hat{\omega} := \omega\sqrt{\frac{Ml^2}{Ml^2 + I}}. \quad (12)$$

The state-space realization of Eq. (12) then becomes

$$\frac{\mathrm{d}}{\mathrm{d}t}\begin{bmatrix} \theta_1 \\ \dot{\theta}_1 \end{bmatrix} = \begin{bmatrix} 0 & 1 \\ \hat{\omega}^2 & 0 \end{bmatrix}\begin{bmatrix} \theta_1 \\ \dot{\theta}_1 \end{bmatrix} + \begin{bmatrix} 0 \\ I/(Ml^2 + I) \end{bmatrix}\ddot{y}_{\mathrm{d}}(t). \quad (13)$$

In the following, we denote Eq. (13) as $\dot{\boldsymbol{x}} = \boldsymbol{A}\boldsymbol{x} + \boldsymbol{B}\ddot{y}_{\mathrm{d}}(t)$.

D. Typical Walking Gaits

Fig. 2 shows the simulation results of steady level dynamic walking where $T_{\mathrm{set}} = 0.7$ [s]. Here, (a) shows the angular positions and the control output in the nonlinear model and (b) shows those in the linearized model. We can see that the linearized model generates stationary orbits very close to those of the nonlinear model.

Fig. 3 shows the time evolutions of the total mechanical energy in the nonlinear model and $E(\boldsymbol{x})$ in the linearized model. We can see that $E(\boldsymbol{x})$ generates a stationary orbit very close to that of the nonlinear model. This is because the only difference between the mechanical energy and $E(\boldsymbol{x})$ is the difference between the potential energies. In every stance phase, from 0 to $T_{\mathrm{set}}/2$, mechanical energy increases because

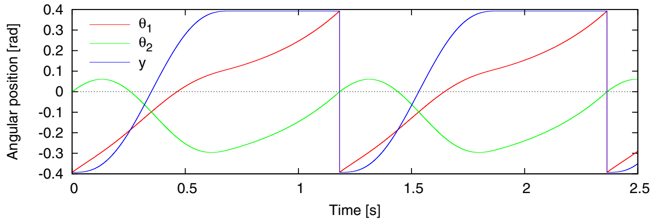

(a) Nonlinear model

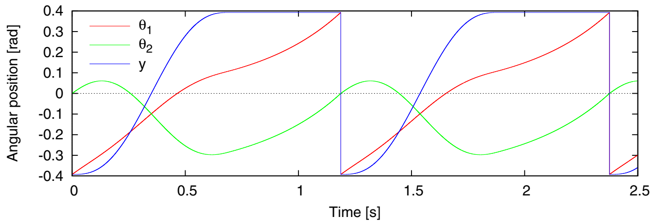

(b) Linearized model

Fig. 2. Time evolutions of angular positions and control output in nonlinear and linearized models

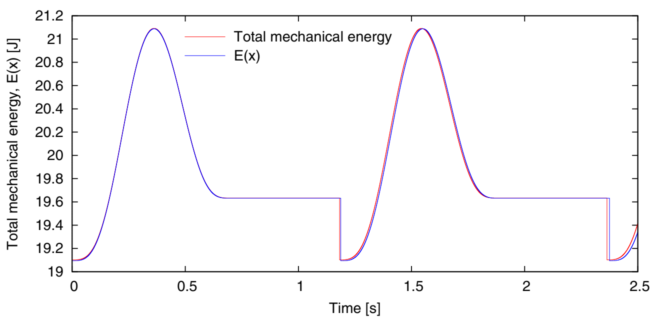

Fig. 3. Time evolutions of total mechanical energy and $E(\boldsymbol{x})$

the control torque accelerates the torso in a counterclockwise direction. Whereas from $T_{\mathrm{set}}/2$ to T_{set}, mechanical energy decreases due to decelerating the torso. After that, the walker moves as a 1-DOF rigid body and the mechanical energy remains constant.

III. DERIVATION OF TRANSITION FUNCTION

A. Recurrence Formula of Kinetic Energy

Let K_i^- [J] be the kinetic energy immediately before the (i)th impact. In a limit cycle walking with constraint on impact posture, the following recurrence formula holds.

$$K_{i+1}^- = \varepsilon K_i^- + \Delta E_i \tag{14}$$

Here, ε [-] is the energy-loss coefficient and satisfies

$$\varepsilon := \frac{K_i^+}{K_i^-} = \frac{\frac{1}{2} I' \left(\dot{\theta}_{1(i)}^+\right)^2}{\frac{1}{2} I' \left(\dot{\theta}_{1(i)}^-\right)^2} = \left(\frac{\dot{\theta}_{1(i)}^+}{\dot{\theta}_{1(i)}^-}\right)^2 = \bar{R}^2, \tag{15}$$

where $I' := Ml^2 + I$ [kg·m^2] is the total moment of inertia about the stance-leg end. ΔE_i [J] is the mechanical energy restored during the (i)th stance phase. In a steady gait, the following equation should hold.

$$K_{\mathrm{eq}}^- = \varepsilon K_{\mathrm{eq}}^- + \Delta E^* \tag{16}$$

Where

$$K_{\mathrm{eq}}^- := \lim_{i \to \infty} K_i^- = \frac{\Delta E^*}{1 - \varepsilon}, \tag{17}$$

$$\Delta E^* := \lim_{i \to \infty} \Delta E_i. \tag{18}$$

Eq. (17) is equivalently arranged to

$$F\left(\dot{\theta}_{1\mathrm{eq}}^-\right) := (1 - \varepsilon) K_{\mathrm{eq}}^- - \Delta E^* = 0. \tag{19}$$

The function F can be expressed as a quadratic equation of $\dot{\theta}_{1\mathrm{eq}}^-$ as follows.

$$F\left(\dot{\theta}_{1\mathrm{eq}}^-\right) = C_2 \left(\dot{\theta}_{1\mathrm{eq}}^-\right)^2 + C_1 \dot{\theta}_{1\mathrm{eq}}^- + C_0 = 0 \tag{20}$$

Here, note that K_{eq}^- is a quadratic equation of $\dot{\theta}_{1\mathrm{eq}}^-$ and ΔE^* is a linear function of it, that is, the following relations hold.

$$(1 - \varepsilon) K_{\mathrm{eq}}^- = C_2 \left(\dot{\theta}_{1\mathrm{eq}}^-\right)^2, \quad \Delta E^* = -C_1 \dot{\theta}_{1\mathrm{eq}}^- - C_0 \tag{21}$$

$\dot{\theta}_{1\mathrm{eq}}^-$ is then derived as the solution of $F\left(\dot{\theta}_{1\mathrm{eq}}^-\right) = 0$, that is,

$$\dot{\theta}_{1\mathrm{eq}}^- = \frac{-C_1 + \sqrt{C_1^2 - 4C_2C_0}}{2C_2}. \tag{22}$$

The quadratic equation (20) has another solution of $\dot{\theta}_{1\mathrm{eq}}^-$, but this is negative and improper.

B. Restored Mechanical Energy for Linearized Model

Let t [s] be the time parameter which is reset to zero at every impact. The state vector for $0^+ \leq t \leq T_{\mathrm{set}}$, $\boldsymbol{x}(t) \in \mathbb{R}^2$, is then determined as

$$\boldsymbol{x}(t) = \mathrm{e}^{\boldsymbol{A}t} \boldsymbol{x}_i^+ + \int_{0^+}^{t} \mathrm{e}^{\boldsymbol{A}(t-s)} \boldsymbol{B} \ddot{y}_{\mathrm{d}}(s) \mathrm{d}s. \tag{23}$$

$\theta_1(t)$ is then obtained by extracting the first element of $\boldsymbol{x}(t)$ in Eq. (23). By considering the following relation:

$$\frac{\mathrm{d}E(\boldsymbol{x})}{\mathrm{d}t} = \dot{\boldsymbol{\theta}}^{\mathrm{T}} \boldsymbol{S} u(t) = \dot{y}(t) u(t) = \dot{y}_{\mathrm{d}}(t) u(t), \tag{24}$$

we can calculate the restored mechanical energy as follows.

$$\begin{aligned} \Delta E_i &= \int_{0^+}^{T_{\mathrm{set}}} \dot{y}_{\mathrm{d}}(s) u(s) \ \mathrm{d}s \\ &= \frac{I \hat{\omega}^2}{\omega^2} \int_{0^+}^{T_{\mathrm{set}}} \dot{y}_{\mathrm{d}}(s) \left(\ddot{y}_{\mathrm{d}}(s) - \omega^2 \theta_1(s)\right) \mathrm{d}s \end{aligned} \tag{25}$$

Here, we can obtain the following.

$$\int_{0^+}^{T_{\mathrm{set}}} \dot{y}_{\mathrm{d}}(s) \ddot{y}_{\mathrm{d}}(s) \mathrm{d}s = \left[\frac{1}{2} \dot{y}_{\mathrm{d}}(s)^2\right]_{s=0^+}^{s=T_{\mathrm{set}}} = 0$$

Eq. (25) then becomes

$$\Delta E_i = -I \hat{\omega}^2 \int_{0^+}^{T_{\mathrm{set}}} \dot{y}_{\mathrm{d}}(s) \theta_1(s) \ \mathrm{d}s. \tag{26}$$

The restored mechanical energy is therefore found to be the integral of the product of $\dot{y}_{\mathrm{d}}(t)$ and the zero dynamics, $\theta_1(t)$. Note that $\theta_1(t)$ is given as a linear function of $\dot{\theta}_{1(i)}^+$, and so is ΔE_i. Specifically, ΔE_i is determined as

$$\begin{aligned} \Delta E_i &= -C_1 \dot{\theta}_{1(i)}^- - C_0 = -C_1 \left(\dot{\theta}_{1\mathrm{eq}}^- + \Delta \dot{\theta}_{1(i)}^-\right) - C_0 \\ &= \Delta E^* - C_1 \Delta \dot{\theta}_{1(i)}^-. \end{aligned} \tag{27}$$

Note that we used the relation $\Delta E^* = -C_1\dot{\theta}_{1\mathrm{eq}}^- - C_0$.

C. Derivation of $\bar{Q}$

The kinetic energy immediately before the (i)th impact can be approximated as follows.

$$\begin{aligned} K_i^- &= \frac{1}{2}I'\left(\dot{\theta}_{1(i)}^-\right)^2 = \frac{1}{2}I'\left(\dot{\theta}_{1\mathrm{eq}}^- + \Delta\dot{\theta}_{1(i)}^-\right)^2 \\ &\approx \frac{1}{2}I'\left(\left(\dot{\theta}_{1\mathrm{eq}}^-\right)^2 + 2\dot{\theta}_{1\mathrm{eq}}^-\Delta\dot{\theta}_{1(i)}^-\right) \\ &= K_{\mathrm{eq}}^- + I'\dot{\theta}_{1\mathrm{eq}}^-\Delta\dot{\theta}_{1(i)}^- \end{aligned} \tag{28}$$

The recurrence formula (14) is then represented as follows.

$$\begin{aligned} K_{\mathrm{eq}}^- + I'\dot{\theta}_{1\mathrm{eq}}^-\Delta\dot{\theta}_{1(i+1)}^- &= \varepsilon\left(K_{\mathrm{eq}}^- + I'\dot{\theta}_{1\mathrm{eq}}^-\Delta\dot{\theta}_{1(i)}^-\right) \\ &\quad + \Delta E^* - C_1\Delta\dot{\theta}_{1(i)}^- \end{aligned} \tag{29}$$

By subtracting Eq. (16) from Eq. (29), we get

$$I'\dot{\theta}_{1\mathrm{eq}}^-\Delta\dot{\theta}_{1(i+1)}^- = \varepsilon I'\dot{\theta}_{1\mathrm{eq}}^-\Delta\dot{\theta}_{1(i)}^- - C_1\Delta\dot{\theta}_{1(i)}^-, \tag{30}$$

and this is arranged to

$$\Delta\dot{\theta}_{1(i+1)}^- = \left(\varepsilon - \frac{C_1}{I'\dot{\theta}_{1\mathrm{eq}}^-}\right)\Delta\dot{\theta}_{1(i)}^-. \tag{31}$$

This means

$$\bar{Q}\bar{R} = \varepsilon - \frac{C_1}{I'\dot{\theta}_{1\mathrm{eq}}^-}. \tag{32}$$

Considering $\varepsilon = \bar{R}^2$ and $\dot{\theta}_{1\mathrm{eq}}^+ = \bar{R}\dot{\theta}_{1\mathrm{eq}}^-$, $\bar{Q}$ can be arranged to

$$\bar{Q} = \bar{R} - \frac{C_1}{I'\dot{\theta}_{1\mathrm{eq}}^+}. \tag{33}$$

IV. STABILITY ANALYSIS

This section discusses the accuracy of the analytical solution of $\bar{Q}$ through comparison with the numerical solutions. We calculate the value of the analytical $\bar{Q}$ according to the following procedure.

(P1) Analytically derive the coefficients C_2, C_1 and C_0.
(P2) Set T_{set} and calculate the values of C_2, C_1 and C_0.
(P3) Calculate $\dot{\theta}_{1\mathrm{eq}}^-$ by using Eq. (22) with C_2, C_1 and C_0 previously obtained.
(P4) Calculate $\bar{Q}$ by using Eq. (33).
(P5) Increase T_{set} and return to (P2).

Whereas in the numerical simulations, we define the real $\bar{Q}$ for the (i)th step, $\bar{Q}_{(i)}$, as

$$\bar{Q}_{(i)} := \frac{\Delta\dot{\theta}_{1(i+1)}^-}{\Delta\dot{\theta}_{1(i)}^+}. \tag{34}$$

In fast convergent gaits, the denominator of Eq. (34) converges to zero as well as the numerator in a few steps, that is, Eq. (34) becomes an indeterminate form. Therefore we calculate the numerical solutions of $\bar{Q}$ for the linearized and the nonlinear models as the mean value for the first three steps:

$$\bar{Q} := \frac{1}{3}\sum_{i=0}^{2}\bar{Q}_{(i)}. \tag{35}$$

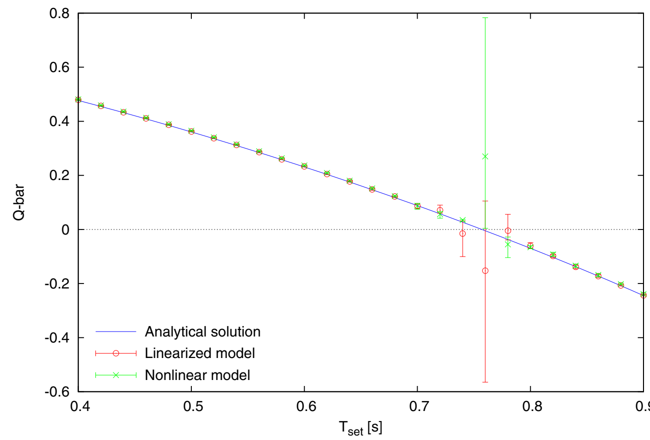

Fig. 4. $\bar{Q}$ and its numerical solutions versus T_{set}

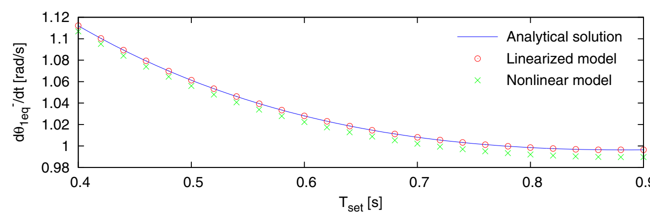

Fig. 5. $\dot{\theta}_{1\mathrm{eq}}^-$ and its numerical solutions versus T_{set}

Fig. 4 plots the analytical $\bar{Q}$ and the numerical ones for the linearized and the nonlinear models with respect to T_{set} where $M = 2.0$ [kg], $l = 1.0$ [m], $I = 1.0$ [kg·m^2]. The initial angular velocity is chosen as $\dot{\theta}_{1(0)}^+ = \dot{\theta}_{1\mathrm{eq}}^+ + 0.01$ [rad/s]. We can see that the accuracy of the analytical $\bar{Q}$ is sufficiently high and the numerical ones tend to diverge near the deadbeat mode.

Fig. 5 plots the analytical $\dot{\theta}_{1\mathrm{eq}}^-$ and the numerical ones for the linearized and the nonlinear models in the previous result. We can see that the analytical $\dot{\theta}_{1\mathrm{eq}}^-$ achieves high accuracy.

V. EXTENSION TO UNDERACTUATED BIPED

A. Problem Formulation

This section discusses the case of a planar underactuated bipedal walker shown in Fig. 6. Since this model has already been used in our previous papers, we omit the details. We assume the followings.

- This walker consists of two identical leg frames with semicircular feet whose radius is r [m] and can exert the hip-joint torque, u_H.
- The walker controls the relative hip-joint angle, $\theta_H := \theta_1 - \theta_2$ to strictly follow the desired-time trajectory, $\theta_{Hd}(t)$, during every stance phase and θ_H moves from -2α to 2α [rad].
- The walker falls down as a 1-DOF rigid body immediately before every impact while keeping the relative hip-joint angle 2α. Then $\theta_1^{\pm} = -\theta_2^{\pm} = \mp\alpha$ always holds at impact.
- The hip joint is mechanically locked during every collision phase.

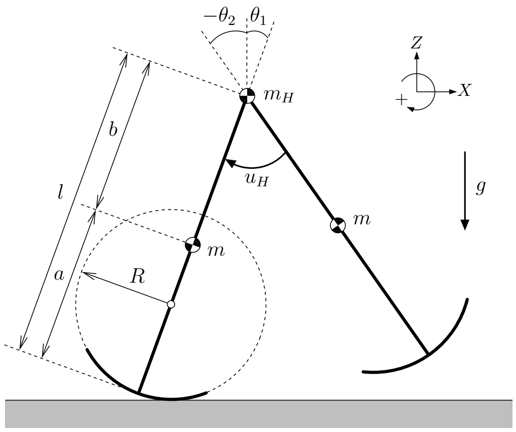

Fig. 6. Model of underactuated biped with semicircular feet

Let $\boldsymbol{\theta} = \begin{bmatrix} \theta_1 & \theta_2 \end{bmatrix}^{\mathrm{T}}$ be the generalized coordinate vector. The equation of motion then becomes

$$\boldsymbol{M}(\boldsymbol{\theta})\ddot{\boldsymbol{\theta}} + \boldsymbol{h}(\boldsymbol{\theta}, \dot{\boldsymbol{\theta}}) = \boldsymbol{S} u_H. \tag{36}$$

By linearizing this about $\boldsymbol{\theta} = \dot{\boldsymbol{\theta}} = \boldsymbol{0}_{2\times 1}$, we get the linearized equation of motion as

$$\boldsymbol{M}_0\ddot{\boldsymbol{\theta}} + \boldsymbol{G}_0\boldsymbol{\theta} = \boldsymbol{S} u_H. \tag{37}$$

Assuming that stance-leg exchange is modeled as an inelastic collision, the transition equation for the angular velocity vector becomes

$$\dot{\boldsymbol{\theta}}_i^+ = \boldsymbol{\Xi}\dot{\boldsymbol{\theta}}_i^- = \boldsymbol{\Xi}\begin{bmatrix} 1 \\ 1 \end{bmatrix}\dot{\theta}_{1(i)}^- = \begin{bmatrix} \xi_1 \\ \xi_1 \end{bmatrix}\dot{\theta}_{1(i)}^-. \tag{38}$$

Note that, however, this is derived by using the nonlinear model. The transition equation for each angular velocity is therefore simply specified as

$$\dot{\theta}_{1(i)}^+ = \dot{\theta}_{2(i)}^+ = \xi_1\dot{\theta}_{1(i)}^-. \tag{39}$$

The transition function of the state error for the collision phase then becomes $\Delta\dot{\theta}_{1(i)}^+ = \xi_1\Delta\dot{\theta}_{1(i)}^-$, that is, $\bar{R} = \xi_1$. This phase is stable because $|\xi_1| < 1$ holds.

The recurrence formula (14) also holds in the generated bipedal gait and the relation $\varepsilon = \xi_1^2 = \bar{R}^2$ thus holds. The total moment of inertia about the origin, I' [kg·m^2], in this case is defined as

$$I' := \begin{bmatrix} 1 \\ 1 \end{bmatrix}^{\mathrm{T}} \boldsymbol{M}(\alpha)\begin{bmatrix} 1 \\ 1 \end{bmatrix}, \quad \boldsymbol{M}(\alpha) := \boldsymbol{M}(\boldsymbol{\theta})|_{\theta_1 = -\theta_2 = \alpha}.$$

Note that $\boldsymbol{M}(\alpha)$ is the inertia matrix of the nonlinear model at impact. The collision dynamics and the kinetic energy immediately before impact need not be linearized and only the restored mechanical energy must be linearized for analytically deriving $\bar{Q}$. The overall walking dynamics is then specified as a LTI system with a switching rule of Eq. (39). We discuss the accuracy of this system through numerical simulations later.

We choose the relative hip-joint angle, $\theta_H = \boldsymbol{S}^{\mathrm{T}}\boldsymbol{\theta}$, as the control output, y. The second-order derivative of y with respect to time becomes

$$\ddot{y} = \boldsymbol{S}^{\mathrm{T}}\ddot{\boldsymbol{\theta}} = \boldsymbol{S}^{\mathrm{T}}\boldsymbol{M}_0^{-1}\left(\boldsymbol{S}u_H - \boldsymbol{G}_0\boldsymbol{\theta}\right),$$

and the control input for achieving $y \equiv y_{\mathrm{d}}(t)$ can be determined as

$$u_H = \frac{\ddot{y}_{\mathrm{d}}(t) + \boldsymbol{S}^{\mathrm{T}}\boldsymbol{M}_0^{-1}\boldsymbol{G}_0\boldsymbol{\theta}}{\boldsymbol{S}^{\mathrm{T}}\boldsymbol{M}_0^{-1}\boldsymbol{S}}, \tag{40}$$

where $y_{\mathrm{d}}(t)$ is the desired-time trajectory for the relative hip-joint angle and is specified as follows.

$$y_{\mathrm{d}}(t) = \begin{cases} \dfrac{24\alpha}{T_{\mathrm{set}}^5}t^5 - \dfrac{60\alpha}{T_{\mathrm{set}}^4}t^4 + \dfrac{40\alpha}{T_{\mathrm{set}}^3}t^3 - 2\alpha & (0 \le t < T_{\mathrm{set}}) \\ 2\alpha & (t \ge T_{\mathrm{set}}) \end{cases} \tag{41}$$

This satisfies the following boundary conditions.

$$y_{\mathrm{d}}(0^+) = -2\alpha, \quad y_{\mathrm{d}}(T_{\mathrm{set}}) = 2\alpha$$
$$\dot{y}_{\mathrm{d}}(0^+) = \dot{y}_{\mathrm{d}}(T_{\mathrm{set}}) = 0, \quad \ddot{y}_{\mathrm{d}}(0^+) = \ddot{y}_{\mathrm{d}}(T_{\mathrm{set}}) = 0$$

By substituting u_H of Eq. (40) into Eq. (37) and arranging it, the state space realization can be specified as $\dot{\boldsymbol{x}} = \boldsymbol{A}\boldsymbol{x} + \boldsymbol{B}\ddot{y}_{\mathrm{d}}(t)$ where

$$\boldsymbol{A} = \begin{bmatrix} \boldsymbol{0}_{2\times 2} & \boldsymbol{I}_2 \\ -\boldsymbol{M}_0^{-1}\left(\boldsymbol{I}_2 - \dfrac{\boldsymbol{S}\boldsymbol{S}^{\mathrm{T}}\boldsymbol{M}_0^{-1}}{\boldsymbol{S}^{\mathrm{T}}\boldsymbol{M}_0^{-1}\boldsymbol{S}}\right)\boldsymbol{G}_0 & \boldsymbol{0}_{2\times 2} \end{bmatrix} \in \mathbb{R}^{4\times 4},$$

$$\boldsymbol{B} = \begin{bmatrix} \boldsymbol{0}_{2\times 1} \\ \dfrac{\boldsymbol{M}_0^{-1}\boldsymbol{S}}{\boldsymbol{S}^{\mathrm{T}}\boldsymbol{M}_0^{-1}\boldsymbol{S}} \end{bmatrix} \in \mathbb{R}^4.$$

B. Restored Mechanical Energy

The mechanical energy corresponding to the linearized model, $E(\boldsymbol{x})$, in this case is also defined in the same form as Eq. (8). The mechanical energy restored by the control input during the (i)th stance phase then becomes

$$\begin{aligned} \Delta E_i &= \int_{0^+}^{T_{\mathrm{set}}} \dot{y}_{\mathrm{d}}(s)u_H(s)\mathrm{d}s \\ &= \int_{0^+}^{T_{\mathrm{set}}} \dot{y}_{\mathrm{d}}(s)\frac{\ddot{y}_{\mathrm{d}}(s) + \boldsymbol{S}^{\mathrm{T}}\boldsymbol{M}_0^{-1}\boldsymbol{G}_0\boldsymbol{\theta}(s)}{\boldsymbol{S}^{\mathrm{T}}\boldsymbol{M}_0^{-1}\boldsymbol{S}}\mathrm{d}s. \end{aligned} \tag{42}$$

As in the case of the previous model, the following equation holds.

$$\int_{0^+}^{T_{\mathrm{set}}} \dot{y}_{\mathrm{d}}(s)\ddot{y}_{\mathrm{d}}(s)\mathrm{d}s = \left[\frac{\dot{y}_{\mathrm{d}}(s)^2}{2}\right]_{s=0^+}^{s=T_{\mathrm{set}}} = 0 \tag{43}$$

Here, note that the following relation

$$\begin{bmatrix} \theta_1 \\ y \end{bmatrix} = \begin{bmatrix} \theta_1 \\ y_{\mathrm{d}}(t) \end{bmatrix} = \begin{bmatrix} \begin{bmatrix} 1 & 0 \end{bmatrix} \\ \boldsymbol{S}^{\mathrm{T}} \end{bmatrix}\boldsymbol{\theta}$$

holds, and this leads to

$$\boldsymbol{\theta} = \begin{bmatrix} \begin{bmatrix} 1 & 0 \end{bmatrix} \\ \boldsymbol{S}^{\mathrm{T}} \end{bmatrix}^{-1}\begin{bmatrix} \theta_1 \\ y_{\mathrm{d}}(t) \end{bmatrix} = \begin{bmatrix} 1 \\ 1 \end{bmatrix}\theta_1 + \begin{bmatrix} 0 \\ -1 \end{bmatrix}y_{\mathrm{d}}(t).$$

ΔE_i is then calculated as follows.

$$\begin{aligned} \Delta E_i &= \boldsymbol{N}\int_{0^+}^{T_{\mathrm{set}}} \dot{y}_{\mathrm{d}}(s)\boldsymbol{\theta}(s)\mathrm{d}s \\ &= \boldsymbol{N}\begin{bmatrix} 1 \\ 1 \end{bmatrix}\int_{0^+}^{T_{\mathrm{set}}} \dot{y}_{\mathrm{d}}(s)\theta_1(s)\mathrm{d}s \\ &\quad + \boldsymbol{N}\begin{bmatrix} 0 \\ -1 \end{bmatrix}\int_{0^+}^{T_{\mathrm{set}}} \dot{y}_{\mathrm{d}}(s)y_{\mathrm{d}}(s)\mathrm{d}s, \end{aligned} \tag{44}$$

where

$$\boldsymbol{N} := \frac{\boldsymbol{S}^{\mathrm{T}}\boldsymbol{M}_0^{-1}\boldsymbol{G}_0}{\boldsymbol{S}^{\mathrm{T}}\boldsymbol{M}_0^{-1}\boldsymbol{S}} \in \mathbb{R}^{1\times 2}.$$

Furthermore, the following equation

$$\int_{0+}^{T_{\mathrm{set}}} \dot{y}_{\mathrm{d}}(s) y_{\mathrm{d}}(s) \mathrm{d}s = \left[\frac{y_{\mathrm{d}}(s)^2}{2}\right]_{s=0+}^{s=T_{\mathrm{set}}} = 0 \qquad (45)$$

holds and thus the second term of the right-hand side in Eq. (44) is zero. Following above, ΔE_i finally becomes

$$\Delta E_i = \boldsymbol{N}\begin{bmatrix}1\\1\end{bmatrix}\int_{0+}^{T_{\mathrm{set}}} \dot{y}_{\mathrm{d}}(s)\theta_1(s)\mathrm{d}s. \qquad (46)$$

The state vector at t [s], $\boldsymbol{x}(t) \in \mathbb{R}^4$, is determined as

$$\boldsymbol{x}(t) = \mathrm{e}^{\boldsymbol{A}t}\boldsymbol{x}_i^{+} + \int_{0+}^{t} \mathrm{e}^{\boldsymbol{A}(t-s)}\boldsymbol{B}\ddot{y}_{\mathrm{d}}(s)\mathrm{d}s,$$

and we can obtain $\theta_1(t)$ by extracting the first element of $\boldsymbol{x}(t)$. We can derive it by using Mathematica in a few minutes.

C. Stability Analysis

Fig. 7 shows the time evolutions of the total mechanical energy of the nonlinear model and $E(\boldsymbol{x})$ of the linearized model in level dynamic walking where $T_{\mathrm{set}} = 0.7$ [s] and $\alpha = 0.2$ [rad]. The robot's physical parameters were chosen as the same as in [3]. We can see that there is a certain amount of error between the two orbits but the amounts of their restorations are almost the same. The maxima of the total mechanical energy and $E(\boldsymbol{x})$ are almost the same but the values before and after impact are a little different. This comes from the difference between the inertia matrices, $\boldsymbol{M}(\boldsymbol{\theta})$ and $\boldsymbol{M}_0$. The non-diagonal elements of $\boldsymbol{M}(\boldsymbol{\theta})$ are functions of θ_H and the approximation error becomes larger as θ_H increases.

Fig. 8 plots the analytical $\bar{Q}$ and the numerical solutions with respect to T_{set}. We can see that the analytical solution $\bar{Q}$ shows a high accuracy except the neighborhood of the deadbeat mode. As in the underactuated rimless wheel, the convergence property changes from the speed mode to the totter mode through the deadbeat mode. The author expects that this change tendency can be observed in general underactuated walking gaits.

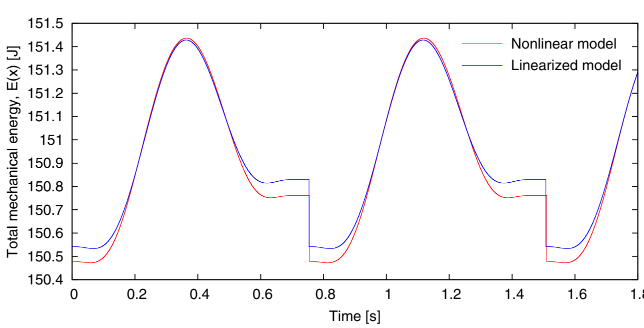

Fig. 7. Time evolutions of total mechanical energy of nonlinear model and $E(\boldsymbol{x})$ of linearized model

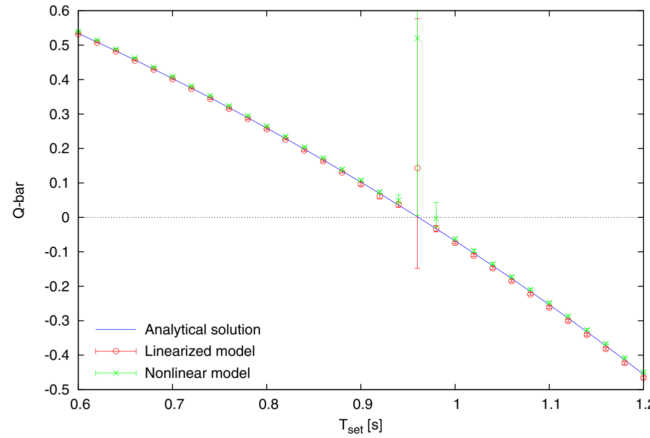

Fig. 8. $\bar{Q}$ and its numerical solutions versus T_{set}

VI. CONCLUSION AND FUTURE WORK

In this paper, we theoretically showed that the stability of limit cycle walking with constraint impact posture can be determined without performing numerical integration. We can easily derive the analytical solution of $\bar{Q}$ by utilizing symbolic manipulation tools such as Mathematica. The simulation results showed that the accuracy of the analytical solutions is sufficiently high.

Now we are attempting to extend the method to multi-DOF models such as a kneed biped. The load of symbolic manipulation would become heavier and finding the solution is left as a future work.

ACKNOWLEDGMENT

This research was partially supported by a Grant-in-Aid for Scientific Research, (C) No. 24560542, provided by the Japan Society for the Promotion of Science (JSPS).

REFERENCES

[1] S. Hosoe, K. Takeichi, S. Kumai, M. Ito, "Analysis of stability of dynamic biped locomotion with high gain feedback," *Trans. of the Society of Instrument and Control Engineers*, Vol. 22, No. 9, pp. 948–954, 1986. (In Japanese)

[2] J. W. Grizzle, G. Abba and F. Plestan, "Asymptotically stable walking for biped robots: Analysis via systems with impulse effects," *IEEE Trans. on Automatic Control*, Vol. 46, No. 1, pp. 51–64, 2001.

[3] F. Asano, "Stability analysis of underactuated bipedal gait using linearized model," *Proc. of the 11th IEEE-RAS Int. Conf. on Humanoid Robots*, pp. 282–287, 2011.

[4] F. Asano and X. Xiao, "Role of deceleration effect in efficient and fast convergent gait generation," *Proc. of the IEEE Int. Conf. on Robotics and Automation*, pp. 5649–5654, 2013.

[5] F. Asano, "Analytical solution to transition function of state error in 1-DOF semi-passive dynamic walking," *Proc. of the IEEE/RSJ Int. Conf. on Intelligent Robots and Systems*, pp. 3114–3119, 2013.

[6] F. Asano and X. Xiao, "Output deadbeat control approaches to fast convergent gait generation of underactuated spoked walker," *Proc. of the IEEE/SICE Int. Symp. on System Integration*, pp. 265–270, 2012.

[7] F. Asano, "Stability principle underlying passive dynamic walking of rimless wheel," *Proc. of the IEEE Int. Conf. on Control Applications*, pp. 1039–1044, 2012.